# 85. Estimation of Dimerisation Constants from Complexation-Induced Displacements of $^1$H-NMR Chemical Shifts: Dimerisation of Caffeine

by **Ian Horman*** and **Bernard Dreux**

*Nestlé* Research Laboratories, CH-1814 La Tour de Peilz

(21.VII.83)

*Summary*

The determination of the dimerisation constant ($K^D$) for the weak self-association of a compound C in dilute solution according to the equilibrium, $2C \rightleftharpoons C_2$ is described. The method uses chemical shifts measured on a series of solutions of C at different concentrations: the optimum $K^D$ is defined by a linear regression best-fit procedure, which simultaneously determines optimum values for $\delta_0$ and also for $\delta_\infty$, the intrinsic chemical shifts for nuclei in the monomer and dimer species. The dimerisation of caffeine in $D_2O$ is used as a model to demonstrate the working of the method and the quality of results obtained. The most probable value of $K^D$ for caffeine at 30.5° is found in the range 5.5–6.0 kg solution $\cdot$ mol$^{-1}$, and the enthalpy and entropy of dimerisation are found to be $\Delta H^\ominus = -15.1$ kJ $\cdot$ mol$^{-1}$ and $\Delta S^\ominus = -35.3$ J $\cdot$ °C$^{-1}$ $\cdot$ mol$^{-1}$, respectively. The influence of small errors in $\delta_0$ on the confidence limits of $K^D$ is discussed.

Weak complexes are important in molecular biology and in pharmacology for interpreting biomechanisms and modes of drug action [1]. Methods to date for determining association constants ($K$) of weak molecular complexes as defined in *Eqn. 1* and *2* have often been approximate, and there have been many reports of anomalous results [2]. We have recently described a method for estimating $K^{AB}$ values as defined in *Eqn. 1* from complexation-induced displacements of NMR line positions in equimolar solutions of the reactants A and B [3]. We report here an improved version of that method and show how it can be applied to study dimerisation according to *Eqn. 2*. Relative to our earlier method, our present approach shows the following advantages: it is about 20 times faster in calculation time, it uses standard linear least-squares statistical methodology, it can be implemented on a relatively modest programmable desk calculator, and it permits the ready estimation of error limits for complex parameters. Further, it retains our rigorous mathematical treatment of the *law of mass action* equation; this we feel is important for the estimation of complex parameters which can be validly compared from one complex to another.

NMR has often been exploited to determine association constants ($K^{AB}$) for weak bimolecular complexes forming according to *Eqn. 1* [4] [5]. Few analoguous determinations of such constants for self-association or dimerisation ($K^D$) as represented by *Eqn. 2* have been reported.

$$A + B \rightleftharpoons AB \text{ for which } K^{AB} = \frac{[AB]}{[A]\,[B]} \tag{1}$$

$$2C \rightleftharpoons C_2 \text{ for which } K^{D} = \frac{[C_2]}{[C]^2} \tag{2}$$

A major reason for this has been that experimental procedures described to date require the direct measurement of $\delta_0$, the intrinsic chemical shift of the uncomplexed species, needed as a reference to determine complexation-induced chemical shift displacements, $(\delta_0 - \delta_i)$. For dimer formation, direct measurement is not possible. At any concentration of C, however small, a quantity of the dimer will always be present, so any measured value of $\delta_i$ for a nucleus in C can never be equal to $\delta_0$. In NMR studies of dimerisation [6] [7], $\delta_0$ has been determined by manual extrapolation of $\delta_i$ *vs.* $[C_i]_0$ curves to zero concentration. Approximate values of $K^D$ have been determined in this manner for the self-association of purine bases in nucleic acids [6] and for the dimerisation of caffeine in $D_2O$ [7]. Our method overcomes this difficulty by estimating $\delta_0$ along with $K^D$ and $\delta_\infty$, optimum values of the three parameters being determined simultaneously by a best fit procedure to the experimental chemical shift *vs.* concentration data. As an example of our method, we present here a detailed study of the dimerisation of caffeine in $D_2O$.

**Theory.** – Starting from the *law of mass action* expression for $K^D$ in *Eqn. 2*, we can write:

$$K^D = [C_2]/([C]_0 - 2[C_2])^2 \tag{3}$$

where $[C_2]$ is the dimer concentration and $[C]_0$ is the nominal concentration of C in solution. Rearrangement of *Eqn. 3* gives:

$$1/2K^D[C]_0 = 2[C_2]/[C]_0 + [C]_0/2[C_2] - 2 \tag{4}$$

But $2[C_2]/[C]_0$ is the fraction of C present as $C_2$, namely the saturation factor [8]. Replacing this by x, and replacing the term on the left of *Eqn. 4* by y, gives *Eqn. 5*, the dimensionless equation of a hyperbola.

$$y = x + 1/x - 2 \tag{5}$$

For a given value of $y_i$, *i.e.*, calculated for a given value of $K^D$ at concentration $[C_i]_0$, *Eqn. 5* is satisfied by two values of $x_i$ which we can call $x_i$ and $x_i^*$, and where $x_i^* = x_i^{-1}$. The value of $x_i$ for which $0 < x_i < 1$, is given by:

$$x_i = (1 + y_i/2) - \sqrt{(1 + y_i/2)^2 - 1} \tag{6}$$

The fraction $x_i$ is related to the measured chemical shift $\delta_i$ through the *Eqn. 7*:

$$x_i = (\delta_0 - \delta_i)/(\delta_0 - \delta_\infty) \tag{7}$$

which on rearrangement gives:

$$\delta_i = \delta_0 - x_i(\delta_0 - \delta_\infty) \tag{8}$$

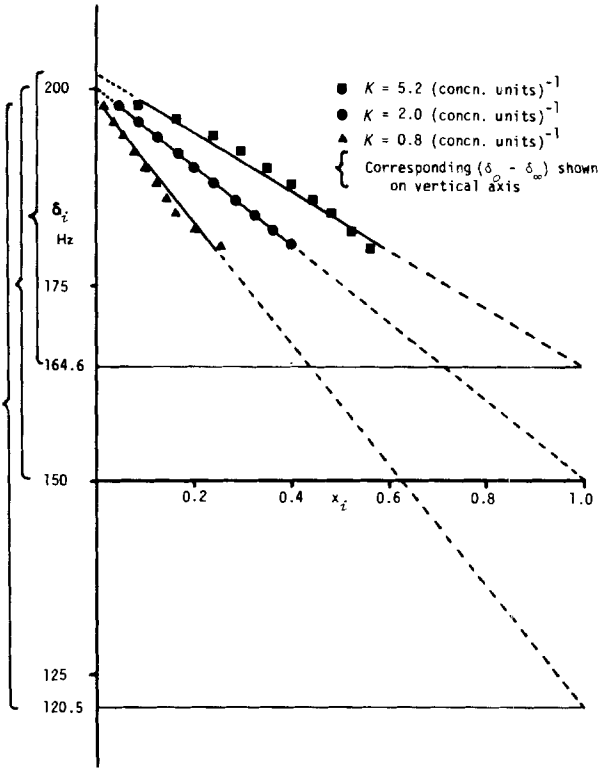


Fig. 1. *Linear regression according to the equation* $\delta_i = \delta_o - x_i \cdot (\delta_o - \delta_\infty)$ *for simulated* ($[C_i]_o$, $\delta_i$) *data created from a hypothetical complex with* $K^D = 2$ *(concn. units)*$^{-1}$, $\delta_o = 200$ *Hz, and* $(\delta_o - \delta_\infty) = 50$ *Hz, showing non-linearity of plots if data is analysed with* $K^D \neq$ *best value*

This is the equation of a straight line relating $\delta_i$ to $x_i$, with slope $-(\delta_0 - \delta_\infty)$ and intercept $\delta_0$. For any given value of $K^D$, a set of $x_i$ values corresponding to the different $[C_i]_0$ concentration in the set of experimental solutions of C can be calculated according to *Eqn. 6*, and plotted against the measured $\delta_i$ as seen in *Fig. 1*, which shows simulated data for a dimer having $K^D = 2$ reciprocal concentration units, $\delta_0 = 200$ Hz, and $(\delta_0 - \delta_\infty) = 50$ Hz. Clearly, for any value of $K^D$ other than the correct one, the plot of *Fig. 1* cannot be linear. In the treatment of real experimental data, the optimum $K^D$ is defined as that value which gives the best straight line fit for $\delta_i$ *vs.* $x_i$. This is readily determined by standard statistical linear regression procedures, and the optimum values for $\delta_0$ and $(\delta_0 - \delta_\infty)$ are determined simultaneously along with $K^D$.

The value of $\delta_0$ calculated is also accompanied by a standard deviation $s(\delta_0)$, which reflects the dispersion in the experimental points. Statistically significant lower and upper limits on $\delta_0$ are given by $\delta_0 - t.s(\delta_0)$ and $\delta_0 + t.s(\delta_o)$, respectively, where t is the *Student*'s coefficient appropriate for the number of experimental points used, and for the level of significance desired. The corresponding limits on $(\delta_0 - \delta_\infty)$ and $K^D$ are obtained by determining the value of $K^D$ which constrains the plot of $\delta_i$ *vs.* $x_i$ to pass through the lower and upper limits of $\delta_0$ as defined above. Values of $\delta$ throughout are expressed as the frequency difference from TMS rather than in ppm. Either convention

could be used, but we chose the former because it is a more convenient unit in which to express minor displacements of peak positions.

**Experimental.** – *Materials.* Caffeine, from *Fluka,* Buchs (CH), was purified by sublimation, m.p. 237° (anh. form) $D_2O$ from *Stohler Isotopes,* Innerberg (CH), was 99.8% isotopically pure, and was used without further purification.

*Methods.* Solutions of caffeine in $D_2O$ were prepared gravimetrically to give a set of solutions $(S_1, S_2, \ldots S_i, \ldots S_N)$ with nominal concentrations $[C_1]_0$, $[C_2]_0$, ... $[C_i]_0$, ... $[C_N]_0$ in the range 0.001–0.1 mol·kg$^{-1}$ solution. $^1$H-NMR spectra were recorded on a *Varian FT-80A* spectrometer at 79.54 MHz and at 30.5° as the average of 100–500 transients depending on the concentration, and chemical shifts for the different nuclei of caffeine (see structure **I**) in the series of solutions were reported either relative to sodium 3-(trimethylsilyl)propionate (TSP) present at the 0.1% level in the experimental solutions, or relative to the signal from a capillary standard containing *s*-trinitrobenzene in $CDCl_3$ and placed coaxially in each successive sample tube. Values of $\delta_i$ for each of the caffeine signals were tabulated along with the corresponding $[C_i]_0$, and these tables became the data files which were treated on a *Hewlett-Packard 3000* computer system, using the iterative program summarized in the flow chart of *Fig. 2,* to calculate best values for the various complex parameters along with their 95% confidence limits.

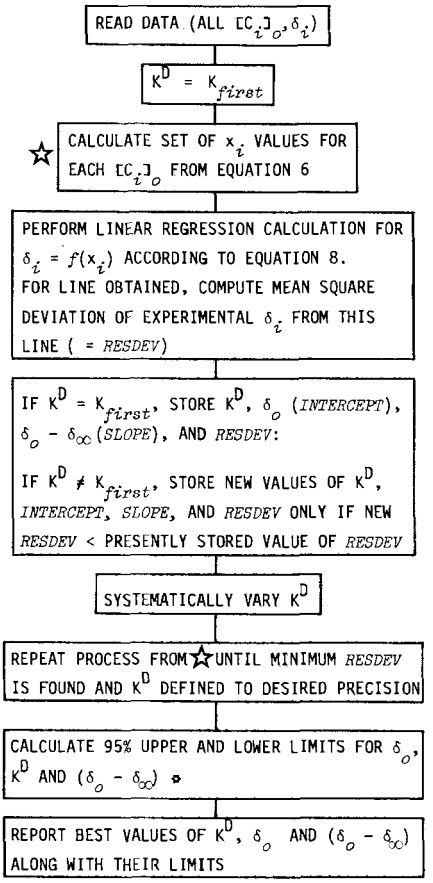


Fig. 2. *Steps in the program used to compute complex parameters.* ☆ $s(\delta_o)$, used in the calculation of 95% limits, is taken as the square root of the average squared residual between measured chemical shifts and the best least squares regression line.

Table 1. *Values of $\delta_o$, $K^D$ and $(\delta_o - \delta_\infty)$ Regenerated by Analysis of Simulated $([C_i]_o, \delta_i)$ Data, Itself Created from Given Sets of Starting Values of the Three Complex Parameters, and with or without Superimposed Errors in $\delta_i$*

| Expt. | Starting values | | | | | Regenerated values | | |
|---|---|---|---|---|---|---|---|---|
| | $\delta_o$ [Hz] | $K^D$ [$c^{-1}$] | $(\delta_o-\delta_\infty)$ [Hz] | No. of data points | Average error in[a]) $\delta_i$ values [Hz] | *min* < $\delta_o$ < *max* | *min* < $K^D$ < *max* | *min* < $(\delta_o-\delta_\infty)$ < *max* |
| 1a | 200.00 | 2.00 | 50.00 | 16 | 0.000 | 200.00 | 2.00 | 50.00 |
| 1b | 200.00 | 2.00 | 50.00 | 11 | 0.086 | *199.87*–200.06–*200.25* | *1.76*–2.20–*2.68* | *42.11*–46.92–*53.57* |
| 1c | 200.00 | 2.00 | 50.00 | 11 | 0.082 | *199.75*–199.92–*200.01* | *1.37*–1.76–*2.20* | *47.38*–54.41–*64.06* |
| 1d | 200.00 | 2.00 | 50.00 | 16 | 0.030 | *199.94*–200.00–*200.07* | *1.82*–1.99–*2.17* | *47.97*–50.03–*52.44* |
| 2a | 200.00 | 2.00 | 20.00 | 16 | 0.000 | 199.99 | 2.00 | 20.01 |
| 2b | 200.00 | 2.00 | 20.00 | 16 | 0.030 | *199.94*–200.00–*200.07* | *1.59*–1.99–*2.44* | *18.09*–20.02–*22.56* |
| 3a | 200.00 | 2.00 | 5.00 | 19 | 0.000 | 200.00 | 1.99 | 5.01 |
| 3b | 200.00 | 2.00 | 5.00 | 19 | 0.051 | *199.86*–199.97–*200.09* | *2.00*–2.88–*3.78* | *3.23*– 5.26– *8.44* |

[a]) Errors in $\delta_i$ superimposed on simulated $\delta_i$ are taken from typical analyses of real experimental sets of data.

**Results.** – *Application to Simulated Data. Table 1* shows the results obtained with simulated data, *i.e.* sets of $([C_i]_0, \delta_i)$ created for hypothetical complexes having predefined values of the three parameters, $K^D$, $\delta_0$, and $(\delta_0 - \delta_\infty)$. To approach reality, we have superimposed typical experimental errors in $\delta_i$, taken from our measurements of actual systems, on the 'perfect' simulated data. Starting values for the complex parameters are compared with those regenerated by our analysis. When no error in $\delta_i$ is introduced (expt. 1a, 2a, 3a) starting values are exactly regenerated: different average errors in $\delta_i$ up to 0.086 Hz, as shown in the other experiments reported in *Table 1*, cause greater or lesser deviations from the starting values, but in all cases these values are included within the 95% limits. However, the smaller the value of the term $(\delta_0 - \delta_\infty)$, the wider become the 95% limits, as seen in expt. 3b where the starting value of $(\delta_0 - \delta_\infty)$ is only 5 Hz.

*Caffeine Dimer.* In the $^1$H-NMR spectrum of caffeine, $CH_3$–N(1) and $CH_3$–N(3) in structure **I** give sharp singlets, $CH_3$–N(7) gives a closely spaces doublet as a result of long-range coupling to H–C(8) ($^4J_{H,H} \simeq 0.6$ Hz), and H–C(8) gives a closely spaced quartet with the same coupling constant.

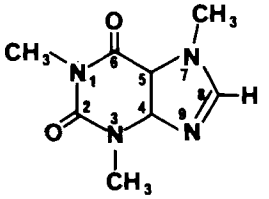


In principle, from a single set of experimental solutions, eight separate sets of $([C_i]_0, \delta_i)$ can therefore be created and used to determine eight corresponding sets of values for the complex parameters. In practice, the outer signals of the H–C(8) quadruplet are too small to be measured accurately, and peak broadening due to sample concentration or minor field inhomogeneities sometimes results in incomplete resolution of

fine structure. *Table 2* shows the results obtained in three separate experiments (experiments are numbered sequentially through the tables). In expt. 5 and 6, the results quoted for $CH_3$–N(7) and H–C(8) are approximate, because $\delta_i$ were taken as average values for the multiplets rather than separating into the individual multiplet components. With few exceptions, values for $K^D$, $\delta_0$ and $(\delta_0 - \delta_\infty)$ in *Table 2* are indistinguishable at the 95% limits of significance.

Table 2. *Complex Parameters for the Formation of the Caffeine Dimer in $D_2O$ at 30.5°*

| Expt. | Concn. range [m/kg soln.] | No. of data points | Protons observed [a] | Optimum calculated complex parameters with 95% limits | | | Average deviation of $\delta_i$ from regression line (Hz) |
|---|---|---|---|---|---|---|---|
| | | | | *min* < $\delta_o$ < *max* [Hz] | *min* < $K^D$ < *max* [kg solution/mol] | *min* < $\delta_o - \delta_\infty$ < *max* [Hz] | |
| 4[b]) | 0.005 | 40 | $CH_3$–N(1) | *267.78*–267.84–*267.91* | *4.97*– 5.30– *5.62* | *24.37*–24.95–*25.60* | 0.033 |
| | –0.075 | 40 | $CH_3$–N(3) | *282.34*–282.40–*282.47* | *5.70*– 6.01– *6.33* | *25.89*–26.37–*26.89* | 0.033 |
| | | 28 | $CH_3$–N(7)a | *315.21*–315.32–*315.43* | *6.00*– 7.11– *8.31* | *12.60*–13.25–*14.09* | 0.054 |
| | | 37 | $CH_3$–N(7)b | *315.84*–315.96–*316.08* | *5.93*– 6.96– *8.06* | *13.43*–14.07–*14.89* | 0.058 |
| | | 31 | H–C(8)a | *628.18*–628.30–*628.42* | *7.80*–12.25–*17.72* | *3.18*– 3.37– *3.76* | 0.058 |
| | | 32 | H–C(8)b | *628.89*–628.98–*629.08* | *8.76*–12.22–*16.19* | *3.64*– 3.82– *4.14* | 0.047 |
| 5[c]) | 0.005 | 20 | $CH_3$–N(1) | *265.73*–265.96–*266.19* | *3.95*– 4.77– *5.65* | *27.58*–29.59–*32.26* | 0.105 |
| | –0.100 | 20 | $CH_3$–N(3) | *280.33*–280.56–*280.78* | *4.65*– 5.43– *6.26* | *28.82*–30.45–*32.51* | 0.107 |
| | | 20 | $CH_3$–N(7) | *313.47*–313.69–*313.91* | *3.86*– 5.03– *6.36* | *17.73*–19.46–*21.94* | 0.105 |
| | | 20 | H–C(8) | *626.18*–626.44–*626.71* | *2.65*– 5.73– *9.74* | *6.77*– 8.05–*11.63* | 0.118 |
| 6[c]) | 0.010 | 20 | $CH_3$–N(1) | *266.05*–266.17–*266.29* | *4.59*– 4.96– *5.34* | *27.81*–28.72–*29.63* | 0.055 |
| | –0.060 | 20 | $CH_3$–N(3) | *280.58*–280.71–*280.83* | *5.35*– 5.71– *6.11* | *28.78*–29.49–*30.19* | 0.056 |
| | | 20 | $CH_3$–N(7) | *313.46*–313.67–*313.88* | *3.52*– 4.50– *5.51* | *17.42*–18.95–*21.32* | 0.096 |
| | | 20 | H–C(8) | *626.63*–626.74–*626.85* | *1.13*– 1.96– *2.99* | *7.70*– 9.15–*13.22* | 0.050 |

[a]) Corresponding to positions in structure **I**.

[b]) Signal positions ($\delta_i$) measured relative to TSP co-dissolved with caffeine at a constant concentration in all solutions of 0.1% w/w.

[c]) Signal positions ($\delta_i$) measured relative to a capillary standard containing *s*-trinitrobenzene/$CDCl_3$.

*Fig. 3* shows plots of chemical shift *vs.* caffeine concentration for the $CH_3$–N(1) and $CH_3$–N(3) signals, and demonstrates the quality of the raw data used in expt. 4, *Table 2*. From this data, different sub-groups of ($[C_i]_0$, $\delta_i$) were created to check the intra-experimental reproducibility of complex parameters calculated. Four sub-groups were chosen as follows: the 40 experimental solutions were numbered in order of increasing concentration; group F (= first) was taken as the 20 lowest concentration points; group L (= last) the 20 highest concentration points; group E (= even) the even numbered points; group O (= odd) the odd numbered points. Complex parameters were then calculated from each sub-groups of 20 points. The values are presented in *Table 3*. With the possible exception of sub-groups $CH_3$–N(1) (L) and $CH_3$–N(3) (L) for which $K^D$ is somewhat low, the overall values compare favourably with each other and with those in expt. 4 coming from all 40 data points.

For comparison with our present results, literature values of $K^D$ and $(\delta_0 - \delta_\infty)$ for the caffeine dimer obtained using manually extrapolated $\delta_0$ values, and reported in [7], are shown in *Table 4*, expt. 7. In this study, the authors presented the complete graphical data of chemical shift *vs.* concentration for the four caffeine signals shown.

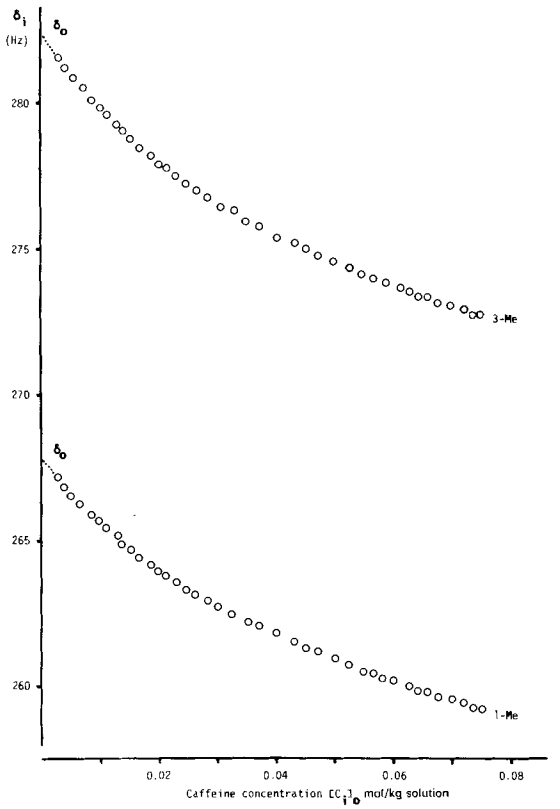


Fig. 3. *Experimental chemical shift* vs. *concentration data for dimer-induced displacements of the* $CH_3$–N(1) *and* $CH_3$–N(3) *peaks of caffeine in* $D_2O$ *at 30.5°*

From photographic enlargements of these graphs, we automatically redigitalised the data to recreate as closely as possible the originally recorded data of ($[C_i]_0$, $\delta_i$). Expt. 8 of *Table 4* shows the results of treating this reconstituted data with our present method. The new values compare more favourably than do those in expt. 7 to the results we report in *Table 2*. In particular, the value of $K^D$ for $CH_3$–N(7) is reduced to less than half that reported from the manually extrapolated $\delta_0$ method.

The evaluation of $\Delta H^{\ominus}$ and $\Delta S^{\ominus}$, the enthalpy and entropy of formation of the caffeine dimer, has been made using the classical *van't Hoff* relationship as shown in *Fig. 4*.

**Discussion.** – The extrapolation of curves beyond the limits between which experimental measurements are feasible is a classical problem of physical chemistry. We have transposed the equation of experimental data curves seen in *Fig. 3* into a linear form which facilitates extrapolation. Clearly, with the calculating power offered by modern computers, we could have used a non-linear regression method directly on the curves of *Fig. 3*, but we have preferred the linear-regression approach for three reasons. *a*) The extrapolation of a straight line is unambiguous; *b*) the approach is perhaps easier to understand in terms of correlating the mathematical operations involved to the physical parameters calculated; *c*) linear least-square regression methods are easy to use, and do not require high-level computing equipment, although evidently, if such equipment is available, the task is further facilitated.

Table 3. *Complex Parameters for the Formation of the Caffeine Dimer Calculated from Sub-groups of Data Created from the Experimental Points for $CH_3$–N(1) and $CH_3$–N(3) Signal Displacements Shown in* Fig. 3

| Expt. | Sub-group[a]) of data points | Concn. range [mol/kg soln.] | No. of data points | Optimum calculated complex parameters with 95% limits | | | Average deviation of $\delta_i$ from regression line (Hz) |
|---|---|---|---|---|---|---|---|
| | | | | *min* < $\delta_o$ < *max* [Hz] | *min* < $K^D$ < *max* [kg solution/mol] | *min* < ($\delta_o - \delta_\infty$) < *max* [Hz] | |
| 4a | $CH_3$–N(1)(F) | 0.005–0.035 | 20 | *267.81*–267.89–*267.97* | *5.02*–5.73–*6.47* | *22.46*–23.92–*25.72* | 0.038 |
| | $CH_3$–N(1)(L) | 0.035–0.075 | 20 | *267.04*–267.09–*267.15* | *3.70*–3.80–*3.90* | *26.72*–26.91–*27.11* | 0.025 |
| | $CH_3$–N(1)(E) | 0.005–0.075 | 20 | *267.71*–267.79–*267.87* | *4.77*–5.13–*5.50* | *24.38*–25.04–*25.79* | 0.038 |
| | $CH_3$–N(1)(O) | 0.005–0.075 | 20 | *267.84*–267.88–*267.93* | *5.41*–5.64–*5.88* | *23.74*–24.12–*24.53* | 0.021 |
| 4b | $CH_3$–N(1)(F) | 0.005–0.035 | 20 | *282.35*–282.43–*282.51* | *5.55*–6.21–*6.89* | *24.64*–25.97–*27.54* | 0.038 |
| | $CH_3$–N(1)(L) | 0.035–0.075 | 20 | *281.42*–281.47–*281.53* | *4.06*–4.16–*4.26* | *28.54*–28.71–*28.90* | 0.027 |
| | $CH_3$–N(1)(E) | 0.005–0.075 | 20 | *282.31*–282.39–*282.47* | *5.49*–5.83–*6.14* | *26.19*–26.74–*27.34* | 0.038 |
| | $CH_3$–N(1)(O) | 0.005–0.075 | 20 | *282.37*–282.42–*282.46* | *6.00*–6.20–*6.41* | *25.69*–26.01–*26.37* | 0.020 |

[a]) Data points of expt. 4 for $CH_3$–N(1) and $CH_3$–N(3) signal displacements ranked sequentially in order of concentration: (F) = 20 lowest concentration points; (L) = 20 highest concentration points; (E) = even numbered points; (O) = odd numbered points.

Earlier methods which employ directly measured $\delta_0$ values [4–7] have implicitly assumed that this quantity is measured with no error, and have used it as a 'perfect' reference point in determining ($\delta_0 - \delta_i$) values and hence complex parameters. Our average error in measuring chemical shifts is about 0.06 Hz, with maximum errors of about 0.3 Hz, and we could expect to have similar errors in the direct measurement of $\delta_0$. Assuming this to be the case, we have determined the effect of this error on the value of $K^D$ estimated from simulated ($[C_i]_0$, $\delta_i$) for a complex having $K^D = 2$ reciprocal concentration units and with ($\delta_0 - \delta_\infty$) = 50 Hz, 20 Hz or 5 Hz. *Fig. 5* shows that the

Table 4. *Literature Values from* [6] *of* $K^D$ *and* ($\delta_o - \delta_\infty$) *for Formation of the Caffeine Dimer in $D_2O$ at 30°* (exp. 7), *and Values of Complex Parameters Calculated with the Present Method from the Corresponding Literature Peak Displacement* vs. *Caffeine Concentration Data*

| Expt. | Concn. range [mol/l soln.] | No. of data points | Protons observed | Optimum calculated complex parameters | | | Average deviation of $\delta_i$ from regression line [Hz] |
|---|---|---|---|---|---|---|---|
| | | | | *min* < $\delta_o$ < *max*[a]) [Hz] | *min* < $K^D$ < *max*[b] [l solution/mol] | *min* < ($\delta_o - \delta_\infty$) < *max*[a]) [Hz] | |
| 7 | 0.005 | | $CH_3$–N(1) | | 5.3 | 30.0 | |
| | – 0.100 | | $CH_3$–N(3) | | 7.4 | 29.5 | |
| | | | $CH_3$–N(7) | | 12.5 | 17.0 | |
| | | | H–C(8) | | 9.3 | 9.0 | |
| 8 | 0.005 | | $CH_3$–N(1) | *302.59*–303.04–*303.49* | *5.69*–7.34– *9.21* | *26.58*–28.15–*30.43* | 0.166 |
| | – 0.100 | | $CH_3$–N(3) | *317.62*–318.02–*318.42* | *4.79*–6.01– *7.37* | *31.17*–33.17–*35.90* | 0.139 |
| | | | $CH_3$–N(7) | *350.63*–351.25–*351.87* | *2.93*–5.62– *9.26* | *18.32*–21.17–*27.74* | 0.233 |
| | | | H–C(8) | *666.08*–666.30–*666.52* | *6.15*–8.39–*11.02* | *9.55*–10.14–*11.06* | 0.077 |

[a]) Corrected from 100 MHz to equivalent values on an 80 MHz instrument to allow comparison with data in *Table 2* and *3*.

[b]) Because concentration units are in mol/l solution, $K^D$ values reported should be divided by approximately *1.1*, namely the density of $D_2O$, to permit comparison with data in *Table 2* and *3*.

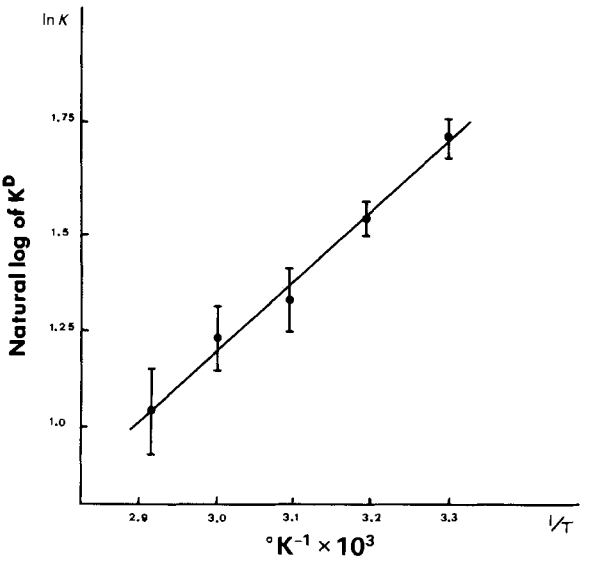


Fig. 4. Van't Hoff *plot from* $K^D$ *values measured at different temperatures and from which the enthalpy and entropy of caffeine dimerisation are estimated.* The natural log of $K^D$ is plotted with 95% limits. $\Delta H^\ominus = -15.1$ kJ · mol$^{-1}$ and $\Delta S^\ominus = -35.3$ J · °C$^{-1}$ · mol$^{-1}$.

error in $K^D$ induced by a minor error in $\delta_0$ is remarkably large and increases markedly as the term $(\delta_0 - \delta_\infty)$ becomes smaller. Error limits for complex parameters reported to date where this effect has not been taken into account should be treated with caution. The correct estimation of error limits associated with different methods is important, particularly in any discussion of anomalous results.

Although the average error in $\delta_i$ in *Table 2–4* is generally better than 0.1 Hz, the limits of incertitude induced in $K^D$ is surprisingly large. This emphasises the need for the careful preparation of experimental solutions and for their subsequent measurement. Like any statistical extrapolation method, precision is favoured by using more data points, and by employing a wide enough concentration range to ensure that the average error in $\delta_i$ is as small as possible when compared to the total range of $\delta_i$ measured. When the range of $\delta_i$ is limited as a result of low values of $K^D$ or $(\delta_0 - \delta_\infty)$, or because of limited solubility, the only way to improve accuracy is to increase the number of data points.

The results for the complex parameters of the caffeine dimer presented in *Table 2–4* need little comment. In all experiments, the best values of $K^D$ estimated from displacements of the $CH_3$–N(1) and $CH_3$–N(3) signals are quite consistent, and the same is true for the corresponding values of $(\delta_0 - \delta_\infty)$. Complex parameters calculated from the $CH_3$–N(7) and H–C(8) signals show greater variations, but there are two reasons for this. Firstly, only expt. 4 shows results where the chemical shifts for the individual components of the multiplets in these signals were measured. The other values corresponding to these signals in expt. 5–8 can thus be looked upon as approximate. This probably also explains why $K^D$ from $CH_3$–N(7) in the literature values presented in expt. 7, *Table 4*, is exaggeratedly high. Secondly, $(\delta_0 - \delta_\infty)$ is lower for the $CH_3$–N(7) and H–C(8) signals, and this restricts the range of $\delta_i$ values. This is the most likely reason for the variability of complex parameters based on displacements of the H–C(8) signal. *Table 3* demonstrates the intra-experimental reproducibility of results. Here, it is

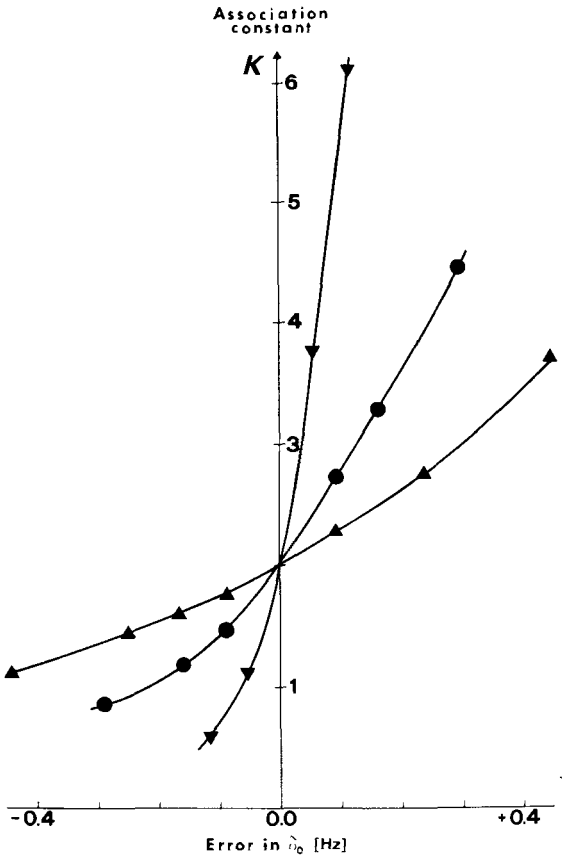


Fig. 5. *The variation of calculated values of* $K^D$ *induced by small errors in* $\delta_o$, *as determined from simulated data for dimer complexes where* $K^D = 2$ *(concn.) and* $(\delta_o - \delta_\infty) = 50$ *Hz* (△); *or 20 Hz* (○); *or 5 Hz* (▽)

normal to see that when the range of concentrations measured is limited, as in the F and L series, the quality of the results declines. Finally, the results from literature data when treated by the present method, fall perfectly into place with our own results as witnessed in expt. 8, *Table 4*.

The *van't Hoff* plot of *Fig. 4* exhibits a good linear relationship, and as such supports the quality of the association constants calculated at different temperatures. The enthalpy and entropy values are typical of charge transfer complexes [9]. $\Delta H^{\ominus}$ is about an order of magnitude stronger than for a *van der Waal's* interaction, about an order of magnitude weaker than for a hydrogen bond interaction, and almost two orders of magnitude weaker than for a $\sigma$-bond. This characterizes the caffeine dimer as a weak $\pi$-bonded molecular complex.

The present work adds to the methodology in quantising weak complexation phenomena, and opens up new possibilities for investigation in a field which has thus far been little explored.

## REFERENCES

[1] *A. Szent-Gyorgyi,* 'Introduction to a Submolecular Biology', Academic Press, New York–London, 1960.
[2] *R. Foster,* 'Organic Charge Transfer Complexes', Academic Press, London, 1969, p. 157.
[3] *I. Horman & B. Dreux,* Anal. Chem. *55,* 1219 (1983): *I. Horman & B. Dreux,* Anal. Chem. *56,* 299 (1984).
[4] *R. Foster,* 'Organic Charge Transfer Complexes', Academic Press, London, 1969, Chap. 6, p. 125 and Chap. 7, p. 179; *R. Foster,* 'Molecular Complexes', Vol. 2, ed. R. Foster, Elek Science, London, 1974, Chap. 3, p. 107; *R. Foster & C. A. Fyfe,* Trans. Faraday Soc. *61,* 1626 (1965).
[5] *M. W. Hanna & A. L. Ashbaugh,* J. Phys. Chem. *68,* 811 (1964); *A. A. Sandoval & M. W. Hanna,* J. Phys. Chem. *70,* 1023 (1966).
[6] *B. W. Bangerter & S. I. Chan,* J. Am. Chem. Soc. *91,* 3910 (1969).
[7] *A. L. Thakkar, L. G. Tensmeyer, R. B. Hermann & W. L. Wilham,* Chem. Commun. *1970,* 524.
[8] *D. A. Deranleau,* J. Am. Chem. Soc. *91,* 4044 (1969).
[9] *R. Foster,* 'Organic Charge Transfer Complexes', Academic Press, London, 1979, Table 7.13, p. 210.